Journal of Applied Sciences

ISSN 1812-5654

science alert

ANSInet
an open access publisher
http://ansinet.com

Journal of Applied Sciences 7 (16): 2261-2271, 2007
ISSN 1812-5654

Application of Optical Methods in Nuclear Track Measurements

[1]Ali Mostofizadeh, [1]Xiudong Sun and [2]Mohammad Reza Kardan
[1]Department of Physics, Harbin Institute of Technology, Harbin 150001, China
[2]Department of Radiation Protection,
National Regulatory Authority Organization, Tehran, Iran

Abstract: In recent years, many theoretical and experimental studies have been carried out to develop one of the most interesting branches of nuclear science called trackology. One of the most attractive aspects of such researches is the investigation of optical properties of nuclear tracks. This field of researches is particularly attractive because it can demonstrate a significant relationship between applied modern optics and nuclear track evaluations. This review paper attempts to summarize some advanced theoretical and experimental methods applied in modern optics to develop some technical skills used in nuclear track studies. Some optical models have been introduced to describe the process of tracks appearance in solid state detectors. Moreover, the theoretical principles of light transmission through the polymeric detectors have been described and some features of Fourier optics have been demonstrated. The practical and experimental aspects of the subject including the applications of coherent light in nuclear track evaluations have been also noticed. In this review, a particular study field in modern optics has been described which can be called optics of nuclear tracks.

Key words: Track measurements, solids, polymeric detector, modern optics, light scattering, He-Ne laser, ECE

INTRODUCTION

One of the most important applications of Solid State Nuclear Track Detectors (SSNTDs) is the use of them in registration of heavy charged particles and neutron (Fleischer *et al*., 1975; Durrani and Bull, 1987). Shape, size, count and orientation of etched tracks can represent us much information about the characteristics of initial incident particles such as incidence angle, energy, flux and occasionally radiation dose. The primary particle trajectories as latent tracks can be observed using optical microscopes after conventional Chemical Etching (CE) (Price and Walker, 1962). Calibrated optical microscopes with sufficient magnification are usually applied to evaluate nuclear track characteristics. Up to now, many studies have been carried out to avoid some problems which occasionally occurred especially whenever optical data collection is only based on light transmission through the SSNTDs. Consequently, losing of optical information due to disregarding scattered beams is occasionally unavoidable. Assuming nuclear tracks act as diffractive apertures, some researchers have focused their studies on applying modern optics to improve nuclear track evaluations.

Historically, some researchers such as Fews (1986), Heinrich *et al*. (1988) and Skvarč *et al*. (1992) have applied the average grey levels and light intensity of images of individual tracks to resolve some problems occurred in tracks recognition due to technical deficiencies of the ordinary light microscopes. Skvarč followed his studies to develop simulation of the process of etching (Skvarč, 1999) based on studies of Ditlov (1995) on tracks calculation in plastics. On the other hand, Ilić and Najer (1990a,b,c) focused their studies on the principle mechanisms of image formation in SSNTDs applying the Babinet's principle. Then, Groetz *et al*. (1998) proposed a new method to improve tracks-etch reading, using the He-Ne laser beam scattered by CR-39. Subsequently, he extended his work in 1999 (Groetz *et al*., 1999), although it seems that during the Groetz's (1999) study, he has comprehensively followed up his own Ph.D thesis at the university of Franche-Comté in 1997. The Groetz's suggestions were applied by Al-Sàad and Abbas (2001) to evaluate the relationship between transmitted He-Ne laser light through the two different kinds of SSNTDs and the etching duration for neutrons and alpha particles. On the other hand, Palacios *et al*. (2001) attempted to apply an alternative method based on Fourier optics to evaluate nuclear tracks in SSNTDs and in another advance in this field, many researchers such as Petford and Miller (1990, 1992), Meesen and Van Oostveldt (1997), Jakes *et al*. (1997), Vaginay *et al*. (2001), Fromm *et al*. (2000 and 2001, 2003), Meesen and Poffijn (2001) and Chambaudet *et al*. (2000), etc., developed various methods based on

Corresponding Author: Xiudong Sun, Department of Physics, Harbin Institute of Technology, Harbin 150001, China

Confocal Laser Scanning Microscopy (CLSM) for further accurately evaluation of nuclear tracks using the high resolution 3-D digital imaging.

Traditionally, the process of visualizing latent tracks in solids is the main step of applying SSNTDs. In view of the growing use of optical methods in SSNTD evaluations, the present study attempts to introduce a part of research activities in this field. In order to this aim, we attempt to describe the optical features of SSNT detectors. As a matter of fact, it is necessary because nuclear tracks are basically the optical phenomena which can be measurable only if their phases change from the latent to the visible state. Furthermore, since the process of etching means visualizing of latent tracks, there is a significant relationship between realizing of the mechanism of etching process and the optical feature of this kind studies.

POLYMERIC DETECTORS

The polymeric nuclear detectors such as Lexan polycarbonate and CR-39 with chemical compositions $C_{16}H_{14}O_3$ and $C_{12}H_{18}O_7$, respectively, are used as the passive detectors, thus against the active detectors they cannot be able to indicate results after measurement, immediately. The essential process called Chemical Etching (CE) (Price and Walker, 1962) and alternatively the electrochemical etching (ECE) (Tommasino, 1970) are two well known methods to enlarge latent tracks. The electrochemical etching process is based on applying an alternative electrical field which can cause electrical treeing breakdown phenomenon at the tip of latent tracks. Furthermore, the enlarged tracks can be observed using optical systems like light microscopes.

Due to many reasons, solid state nuclear track detectors are frequently used to detect charged particles and fast neutrons. In some high level dose areas such as reactor halls and high energy accelerators, workers are not allowed to perform measurements by using of routine detectors, directly. Moreover, in some mixed radiation fields such as an electron field accompanied with neutrons or other particles (e.g., inside the main room of a high energy accelerator) radiation measurements occasionally requires using SSNTDs as the passive detectors. Typical SSNTDs such as Lexan Polycarbonate and CR-39 have commonly very low sensitivity to X-ray and electrons, while they are highly sensitive to heavy charged particles such as α-particles and ions like fission fragments. They have also a good sensitivity for directly registration of fast neutrons while they can be applied as thermal neutron detectors (indirectly) using some converters such as ^{10}B and ^{6}Li with high cross-section for the reaction (n_{th},α). Applying SSNTDs (Tommasino, 1993) requires a wide range of evaluations such as counting, geometrical measurements (e.g., diameter, depth and orientation) and occasionally identification of the initial particle characteristics such as energy and incidence angle which all are estimated by evaluation of tracks appearance in SSNTDs.

OPTICAL MODELS

The appearance of latent tracks: To describe the optical aspects of solid state nuclear track detectors, it is often useful to know the basic knowledge of the physical mechanisms of light scattering and transmission through SSNTDs, however initially we are interested in some physical and chemical phenomena by which the visible track apertures can be formed due to the etching process of initial latent tracks. Therefore, it is necessary to consider appropriate models for simulating of etching process.

A typical appearance of nuclear tracks (α-particle tracks in CR-39) can be observed under a microscope similar to what has been shown in Fig. 1 (Durrani and Bull, 1987). The structure of an individual track can also be described based on a simple model as shown in Fig. 2 (Skvarč, 1999; Ditlov, 1995). In fact, an individual track is a set of circular disks (concentric circles in Fig. 2) over together along the particle trajectory in the polymer's bulk. During the process of etching, each black point on the track wall is extended in a duration time of Δt. Therefore, whole track's volume is grown by two simultaneous rates of v_b and v_t inside the polymer's bulk and along the particle trajectory, respectively.

The simultaneous growing of the whole track along the particle trajectory and inside the polymeric bulk has been shown in Fig. 3, which is due to the continuance of etching after the onset of track appearance (Fromm *et al*., 2003).

Two etching rates v_b and v_t are equal whenever the process of etching continues up to the end of particle

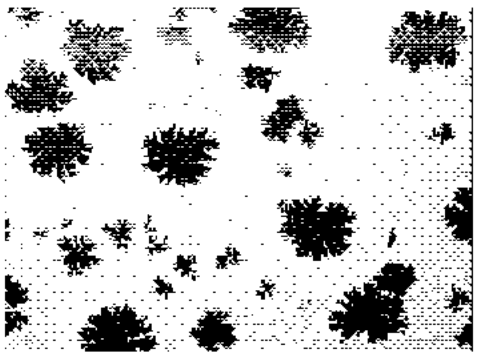

Fig. 1: A typical microscopic image of α -particle tracks in CR-39 (Durrani and Bull, 1987)

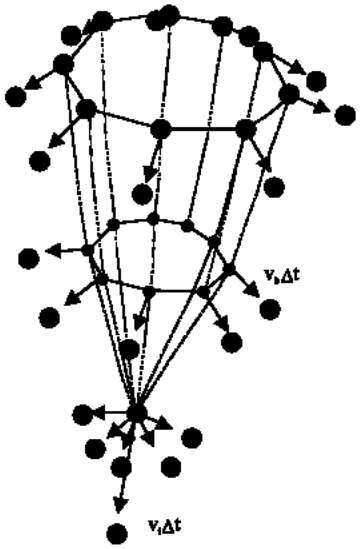

Fig. 2: Growing an individual track during the etching process: v_b indicates the detector's bulk etching rate and v_t is the etching rate along the particle trajectory (Skvarč, 1999)

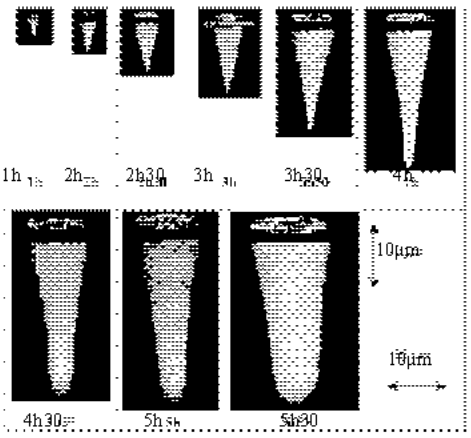

Fig. 3: Different appearances of 3-D lithium-etched tracks under a confocal laser scanning microscope due to increasing of etching time (Fromm *et al*., 2003)

trajectory (Skvarč, 1999), however before this equality occurs, the relationship between two values is written as the following equation (Somogyi *et al*., 1984):

$$v_t(R) = 11.6R^{-0.464}.v_b \quad (1)$$

where, R is the residual particle range in polymer. An etch pit cone can be formed only whenever the etching rate along the particle trajectory is greater than rate of polymer's bulk etching $(\frac{v_t}{v_b} > 1)$.

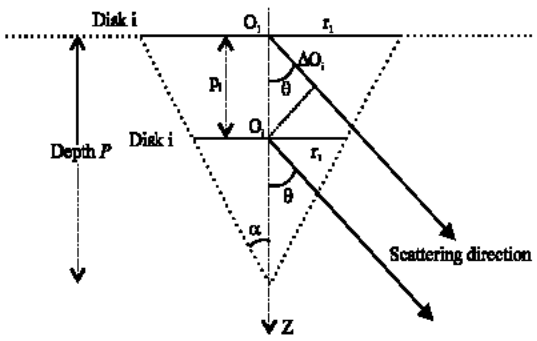

Fig. 4: Geometry of a conical track (Groetz *et al*., 1998)

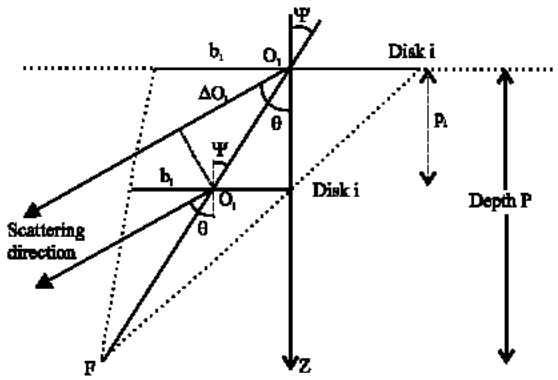

Fig. 5: Geometry of an oblique track (Groetz *et al*., 1998)

Light transmission: The intensity of light scattered by a single track can be defined as the following relation:

$$I_t = |U_t|^2 \quad (2)$$

where, U_t is the distribution of total complex light amplitude scattered by a single track and is calculated by summation of all complex amplitudes (U_i) over the total assumed circular disks around the particle trajectory (Fig. 4 and 5). Therefore, U_t can be calculated as the following summation:

$$U_t = \sum_i U_i \quad (3)$$

In the same manner, one may calculate the light intensity scattered by several etched tracks, however initially one must realize the statistical populations of tracks on a typical SSNTD. The Poisson distribution can be used to define the probability of the number x of tracks inside a population of tracks with the average m tracks per unit area (Groetz *et al*., 1998):

$$P(x) = \frac{m^x}{x!}e^{-m} \quad (4)$$

Consequently, tracks population on a typical SSNTD foil is actually a statistical concept based on a statistical model which represents the probability of an absolute population inside a specific area over the SSNTD surface. It should be proportionally expected that the light intensity scattered by tracks has normally statistical variations on the SSNTD's surface. Nonetheless, we can define the spatial distribution intensity for a particular foil containing a set of etched tracks as the following (Groetz, 1997):

$$I = \sum_t I_t = \sum_t \left| \sum_i U_i \right|^2 \quad (5)$$

where, I_t is total light intensity scattered by each track. On the other hand, the optical density of nuclear tracks on a typical SSNTD can be defined as (Groetz *et al*., 1998):

$$D = \log\left(\frac{I_0}{I}\right) \quad (6)$$

where, I_0 and I are incident and transmitted light, respectively. Moreover, regardless of the radial dependence of light transmission, a particular relationship can be approximately considered between fraction of transmitted light ($T = I / I_0$) and two measurable quantities namely average track density (ρ) and track diameters (2r) as the following (Ilić and Najer, 1990; Groetz *et al*., 1998):

$$T = T_t + (T_f - T_t)e^{-\pi r^2 \rho} \quad (7)$$

where, T_t and T_f are the light transmission through an individual track and through the tracks free area on the SSNTD, respectively. Consequently, the relationship between optical density of an etched SSNTD foil and the average track density is written as follows (Ilić and Najer, 1990; Groetz *et al*., 1998):

$$D = -\log T = -\log\left[T_t + (T_f - T_t)\exp(-\pi r^2 \rho)\right] \quad (8)$$

This model is in fact an informative expression to qualify an alternative optical model for reading solid state nuclear track detectors. Furthermore, when track apertures exposed by coherent light, there are two main phenomena including transmission and reflection in which tracks analysis can be performed using related optical models (Fews, 1992).

Light scattering: Light scattering phenomenon by conical and oblique etched tracks has been schematically shown in Fig. 4 and 5 (Groetz *et al*., 1998). The figure show two angular conditions of the particle incidence to the detector's surface in which the perpendicular and oblique conic tracks can be formed. In both cases, disk 1 is the phase origin (as the initial track aperture on the SSNTD's surface) with respect to i-th disk with depth p_i from the detector's surface. Besides, considering Fig. 4 and 5, in both cases there are optical path differences indicated by ΔO_i which can cause the phase difference between light beams passing through the initial disks 1 and disk i, as the following:

$$\Delta\varphi_i = \exp(jk\Delta O_i) = \exp(jkp_i\cos\theta)\ ;\ \text{Conical tracks}$$
$$\exp\left[jk\frac{\cos(\psi-\theta)}{\cos\theta}p_i\right]\exp(-jkp_i);\ \text{Oblique tracks} \quad (9)$$

where, ψ and θ are the incidence angle of particle and the light scattering angle, respectively. As Groetz *et al*. (1998) have expressed, according to Fraunhofer diffraction formula for a circular aperture, two equations can be written for evaluating the light diffraction by normal and oblique conical tracks. In other words, the well known Fraunhofer formula is generalized for oblique tracks based on Rayleigh-Sommerfeld relation (Born and Wolf, 1959). Consequently, according to Eq. 3, the distribution of total complex light amplitude (U_t) scattered by a single track is calculated as follows (Groetz *et al*., 1998):

$$U_t(\theta) = \sum_i U(\theta, p_i) = \sum_i \frac{1}{j\lambda z}\left[\frac{\pi d_i^2}{2}\frac{J_1(\pi d_i r_0/\lambda z)}{d_i r_0/2\lambda z}\right](\cos\theta)\exp\left[jkp_i(\cos\theta - 1)\right] \quad (10)$$

where, J_i is the first-order Bessel function of the first kind, z is the SSNTD's surface distance from the observation plane and d_i is the diameter of disk i. It should be noticed that complex light amplitude (Eq. 10) is in fact, the summation of all terms of light diffracted by all circular apertures along the particle trajectory (Fig. 5 and compare with Fig. 2).

In the case of non-perpendicular incidence, oblique tracks are formed which are in fact a set of oblique cones which their cross sections with horizontal planes (planes perpendicular to z axis) are a set of elliptical disks with minor and major axes. The minor and major axes should take into account in calculation using an elongation factor defined as the ratio μ = minor axis/major axis (Born and Wolf, 1959). On the other hand, the optical model proposed by Skvarč (1997) for various incident angles allows calculating the fraction of transmitted light through the SSNTDs as the following expression:

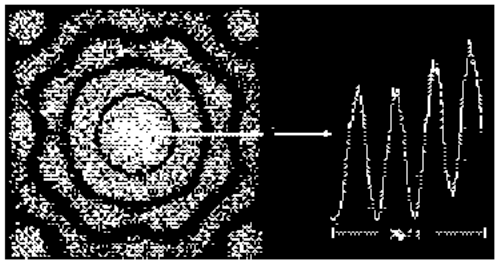

Fig. 6: Fraunhofer diffraction pattern of etched tracks (Left) and distribution of the radial intensity (Right) (Palacios *et al*., 2001)

$$j_t = \frac{1}{2}\left[\left(\frac{2n\cos\varphi_i}{n^2\cos\varphi_i + \sqrt{n^2 - \sin^2\varphi_i}}\right)^2 + \left(\frac{2\cos\varphi_i}{\cos\varphi_i + \sqrt{n^2 - \sin^2\varphi_i}}\right)^2\right]\sqrt{\frac{n^2 - \sin^2\varphi_i}{1 - \sin^2\varphi_i}} \quad (11)$$

where, n is the refraction index of the applied SSNTD. Evidently, considering an incoming cone as the input light to the SSNTD's surface, Eq. (11)? should be computed for all incoming angles (φ_i) for obtaining total transmitted light.

Fourier optics: Fig. 6 (left) shows the well known Fraunhofer diffraction pattern formed due to track apertures exposed by coherent light (Palacios *et al*., 2001). The radial distribution of intensity versus radial position in observation plane is represented in the right part of the same figure. The complete format of radial intensity distribution has been shown in Fig. 7. The section of sinusoidal continuous curve (Fig. 7) has been drawn using Fraunhofer formula and Eq. (2) for an individual track (Palacios *et al*., 2001; Tüke *et al*., 1978):

$$\begin{aligned} I_t(R) &= \left|U_t(R)\right|^2 \\ &= U_t(R)U_t^*(R) = \frac{\lambda f}{4\pi^2 R^3} \\ &\left[D^2 d + D^2 d\cos\left(\frac{2\pi R d}{\lambda f} - \frac{3\pi}{2}\right)\right] \end{aligned} \quad (12)$$

where, R is the polar coordinate in the Fourier plane, d is the track diameter. Besides, λ and f are the light wavelength and focal length of the lens used to observe diffraction pattern, respectively.

The parameter D called optical density in the object plane is, in fact, a non-zero quantity inside [-d/2, d/2] and is given by the inverse Fourier transform of light amplitude distribution as follows (Palacios *et al*., 2001):

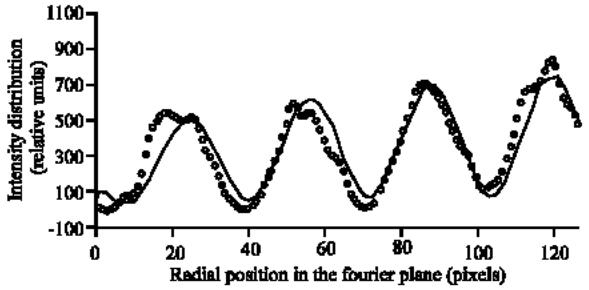

Fig. 7: Radial intensity distribution in the Fourier plane: Theoretical model based on Eq. 12 (continuous curve) and distribution based on software called TRACKS (circles) (Palacios *et al*., 2001)

$$D(r,\theta) = f^{-1}\left\{U(R,\phi)\right\} \quad (13)$$

where, (r, θ) and (R, ϕ) are the polar coordinates in the object plane (SSNTD surface) and observation plane, respectively. Consequently, Fourier analysis of diffraction pattern can be applied for accessing some geometrical characteristics of etched tracks as diffractive apertures. If D(r) is Fourier transformative function i.e., U (R) = f {D(r)}, according to the Parseval's theorem it is proved that (Yu, 1983):

$$\int_{-\infty}^{\infty}\left|D(r,\theta)\right|^2 dr d\theta = \frac{1}{4\pi^2}\int_{-\infty}^{\infty}\left|U(R,\phi)\right|^2 dR d\phi \quad (14)$$

Using Eq. 5, for normal population of etched tracks and applying Parseval's theorem (Eq. 14), the Radial intensity distribution can be obtained by Fourier transformation of Eq. 12 for N_t tracks as the following expression (Palacios *et al*., 2001):

$$f\left\{I_{tot}(R)R^3\right\} = \sum_{i=1}^{N_t}\left[\frac{\lambda f}{2\pi}D_i^2 d_i\delta(0) + \frac{\lambda f}{4\pi}D_i^2 d_i\delta\left(\frac{2\pi d_i}{\lambda f}\right)\right] \quad (15)$$

To calculate the equation above, Palacios *et al*. (2001) have used two previously defined Fourier transformations of f {1} = $2\pi\delta$ (0) and f {cos(ω_0t)} = $\pi\delta$ (ω_0). As it has been mentioned by the authors (Palacios *et al*., 2001) based on Eq. 12 and 15, there is an informative relationship between the characteristics of Fourier spectrum and diameter of tracks, so that Palacios *et al*. proposed their method for tracks analysis based on following expressions:

$$I_{tot}(R)R^3 = \sum_{i=1}^{N_T}\sum_{R=1}^{N_P/2} \left\langle Mn_i d_i R^{K_i}\left\{1+\frac{1}{F_i}\cos\left[2\pi d_i\frac{R}{N_p}-\frac{3\pi}{2}\right]\right\}\right\rangle \quad (16)$$

$$f\left\{I_{tot}(R)R^3\right\} = \sum_{i=1}^{N_T}\left[I_0^N\delta(0)+I_{P_i}^{N_i}\delta(d_i)\right] \quad (17)$$

The parameters used by two equations above have been defined as the following (Palacios *et al*., 2001):

n_i : No. of tracks on SSNTD with diameter d_i.
N_p : No. of image pixels.
N_T : The classes of tracks.
K_i : Background.
F_i : Factor related to track form.
M : Proportional constant obtained by experiment.
I_0^N : The harmonic amplitude of zero order.
$I_{P_i}^{N_i}$: The secondary harmonic amplitude.

Equation 16 and 17 demonstrate a linear relationship between number of tracks which have diameter d_i (n_i) and the secondary harmonic amplitude ($I_{P_i}^{N_i}$). Figure 7 compares the light intensities calculated by Eq. 12 and the radial intensity based on specific computer software called TRACKS (Palacios *et al*., 2001). All parameters applied in Eq. 16 and 17 have been also obtained using the program TRACKS developed by the authors (Palacios *et al*., 2001).

PRACTICAL ASPECTS

Coherent light application in nuclear track evaluations: A new method has been introduced by Groetz *et al.* (1998) to improve the reading of SSNTDs commercially called CR-39. In Groetz's study, a He-Ne laser with the wavelength 632.8 nm and power of 10 mW was used as a coherent light source. Then the angular distribution of the scattered light intensity was measured by a silicon photodiode as a light detector at a distance of 10 cm from the etched CR-39 foil. The SSNTD used by the researchers (CR-39 with chemical composition $C_{12}H_{18}O_7$) is transparent so that its refractive index (1.493 for λ = 633 nm) is close to the value of glass. Therefore, because of a high signal-to-noise ratio for the reflective light, Groetz *et al.* (1998) ignored the reflection mode. On the other hand, red coherent light (λ = 633 nm) has been chosen for minimizing light absorption in CR-39. Samples were exposed by 120 to 2000 keV protons (10^4 to 10^6 protons/cm^2) accelerated by a van de Graaff in three specific incidence angles (0°, 10° and 20°). The proportion of transmitted to incoming light intensity (I/I_o) for three irradiation angels 0°,10° and 20° has been shown in Fig. 8a-f. As the figures show, in the case of perpendicular incidence (protons incidence angle equal to 0°) the curves of I/I_o versus light scattering angle have symmetrical shapes around the zero scattering angle (0°). Therefore in the mentioned case, tracks have circular shapes in two perpendicular measurement plans (a, b); However, Fig. 8a-f show that the symmetrical condition is gradually changed in the case of diagonal proton incidence (10° and 20°) in which oblique tracks are created. In the other part of Groetz's study, some optical models described in this article have been applied to calculate the light amplitude for conical and spherical etched tracks. Calculations for the case of normal incidence were performed based on determination of all parameters required in Eq. 10. Depth of tracks (p) inside polymer was randomly chosen using a computer code for simulating of etching process based on a Ph.D thesis at university of Franche-Comté in 1996 (Groetz *et al*., 1998). Moreover, diameters of circular apertures were also chosen randomly based on diameter measuring of real tracks using a calibrated microscope. Fig. 9a-c show the curves of I/I_0 ratios versus scattering angle for real tracks and simulated tracks with two mean diameters of 5.78 and 4.10 μm, respectively. The figures show that for scattering angles less than 50°, there is a sufficient accordance between the curves associated with calculations and experiments, whereas the Fig. 9d shows that such a mentioned accordance is not satisfactorily observed for tracks with a mean diameter of 2.89 μm. According to authors' expression, such a difference between calculation and experiment results, is basically observed for apertures with diameters less than 2.89 μm. In addition, comparable results are given using similar models for the case of light scattering by oblique tracks in different incidence angles (Groetz *et al*., 1998). In the models used to describe light scattering by oblique tracks, the elongation factor of tracks (μ = minor axis /major axis) should be randomly chosen based on impact angles. However, in the Groetz's studies, the regularity observed in the curves related to calculation models cannot be observed as well as the experiments. As authors have mentioned, disregarding of some effective parameters has caused this disagreement between calculation and experiment results (Groetz *et al*., 1998). Some approximations like insufficient number of tracks used in calculations (less than 1000 tracks), tracks shape simplicity assumed in their simulation models and negligence from the polarization effect, all have affected the Groetz's studies.

On the other hand, as Groetz *et al.* (1998) reported four mean amounts of the aperture diameters (6.22, 5.78,

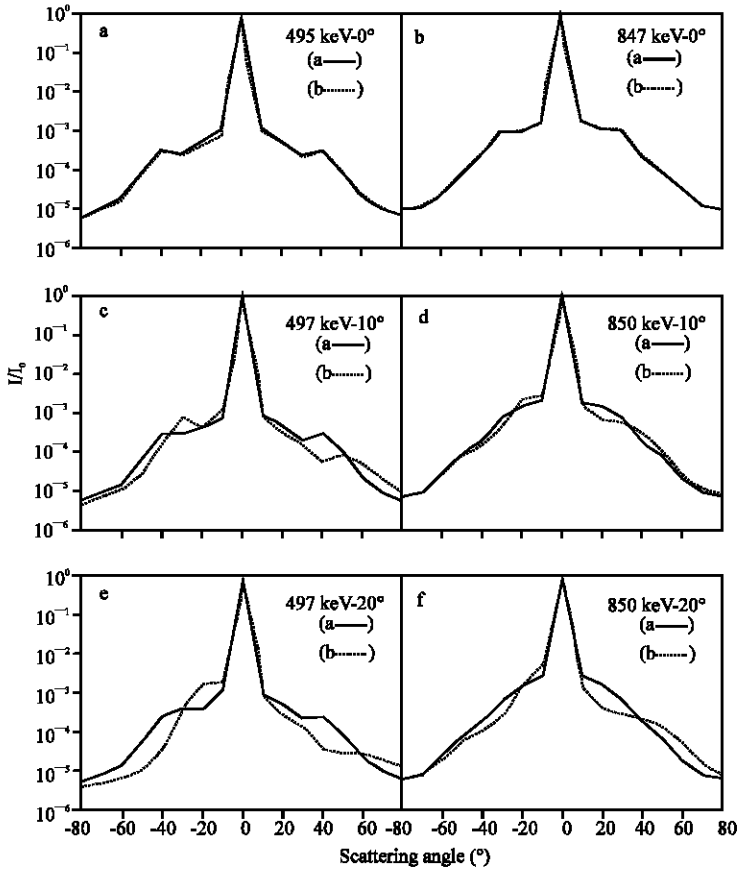

Fig. 8: The proportion of I/I_0 versus scattering angle in deferent proton incidence angles: (a) 495KeV (0°), (b) 847KeV (0°), (c) 497 (10°), (d) 850KeV (10°), (e) 497 (20°) and (f) 850KeV (20°) (Groetz *et al*., 1998)

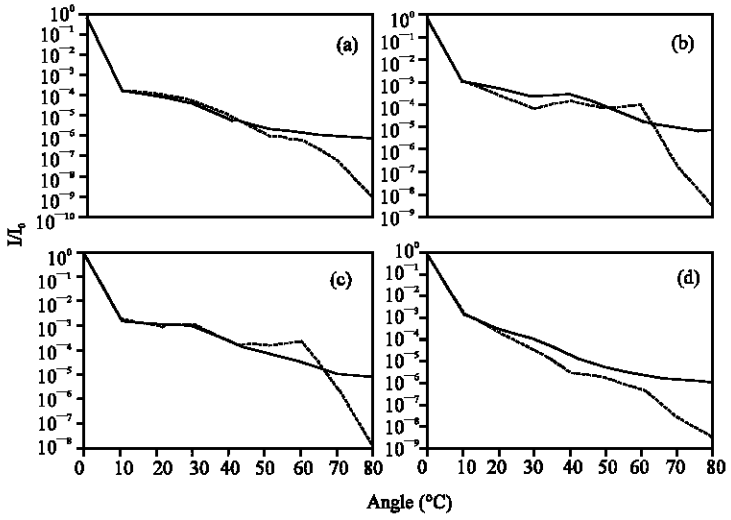

Fig. 9: Comparison between experimental (solid lines) and calculations (dashed lines) of I/I_0 ratio versus scattering angle for perpendicular incidence of the particles (conical tracks). The average diameters of simulated aperture (tracks): (a) 6.22 μm, (b) 5.78 μm, (c) 4.10 μm and (d) 2.89 μm (Groetz *et al*., 1998)

4.10 and 2.89 μm) with two decimal digits. It is clear that real track diameters are not estimable by an ordinary microscope, therefore reporting two significant decimal digits for the mean amounts of track diameters cannot be logical.

In recent years, the Los Alamos National Laboratory (LANL) and the Georgia Institute of Technology (GA-Tech) in USA have designed two Laser Illuminated Track Etch Scattering (LITES) devices for personnel neutron dosimetry (Moore *et al*., 2002). The new feature of the system mentioned by the authors is using a laser mask to prevent full power beam of laser impinges on the surface of photo-detector. Therefore, Moore *et al*. (2002) have avoided locating the detector out of the symmetry axis of the optical system. Furthermore, locating a lens after SSNTD has caused refocusing the scattered light on the photo-detector and consequently increasing the sensitivity of the system. The authors used two deferent Labs (the Pacific Northwest National Lab and the Los Alamos National Labs) to irradiate the sets of CR-39 foils with both a bare ^{252}Cf and a D_2O moderated ^{252}Cf neutron fields. They used a same etch protocol for chemically etching of all irradiated foil sets (Moore *et al*., 2002).

Grey level evaluation: In 1999, Skvarč applied a computer simulation model to evaluate some optical properties of nuclear tracks (Skvarč, 1999). This track visualization model tried to determine average grey levels inside each track to compare the geometric details obtained by computer simulation and experiments. In the experimental part of this work, CR-39 foils were irradiated by 5.15 MeV alpha particles of ^{239}Pu in different incidence angles. Figure 10a and b show the appearance of tracks observed under a microscope and tracks simulated by computer, respectively. The process of tracks enlargement has occurred under a same etching condition but for different incidence angles. The figures show track shape variations with respect to incidence particles angle (from top to bottom: 0°,10°...60°) and the etched out thickness associated to etching duration (from left to right: 3.5, 5.9, 8.5, 11.0, 13.9, 15.8, 18.5 and 20.9 μm). Central average grey levels for real tracks and simulated tracks versus removed CR-39 thickness have been shown in Fig. 11. As shown in this figure, there is a proper agreement between the results of track appearance due to experiment and computer simulation (Fig. 10a and b) so that in both cases (real and simulated tracks), regular changes are perfectly observed in related grey levels with respect to removed thickness and incidence angle. This agreement between central grey levels of real and simulated tracks has also been observed considering two curves shown in Fig. 11.

Furthermore, the phenomenon of tracks obliquity has been shown in the pictorial results shown in Fig. 10,

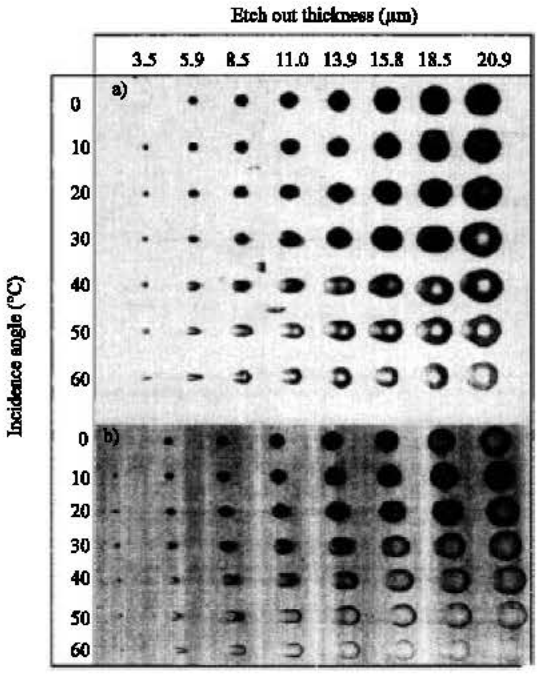

Fig. 10: Tracks-etch appearance at various incidence angles (top to below) and etched out thicknesses (left to right) related to etching time for (a) real tracks and (b) simulated tracks (Skvarč, 1999)

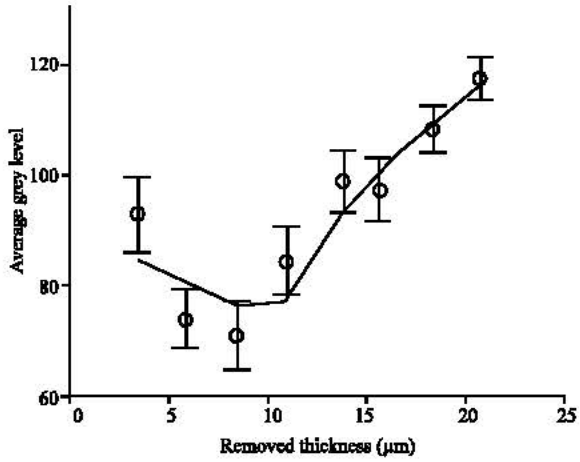

Fig. 11: The average grey levels of real etched tracks (points) and simulated tracks-etch (solid line) (Fig. 4) versus removed thickness of CR-39 (Skvarč, 1999)

thus in normal incidence (0°) track shapes in all etched out thicknesses are evidently circular. However, track features have been gradually changed from the circular to elliptic shapes due to non-perpendicular incidence. As

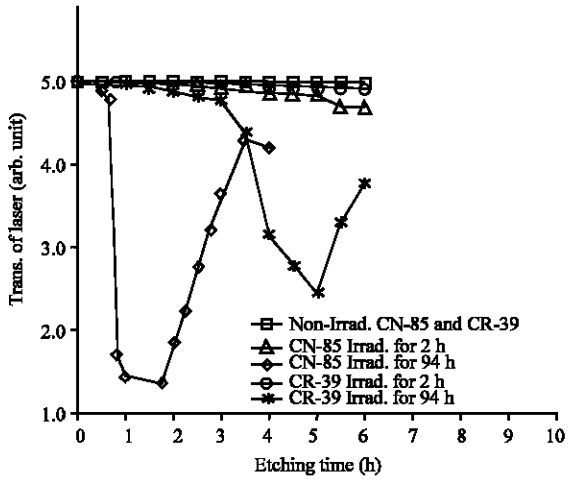

Fig. 12: Transmission of laser light through the SSNTD's irradiated by α-particles (Al-Saad and Abbas, 2001)

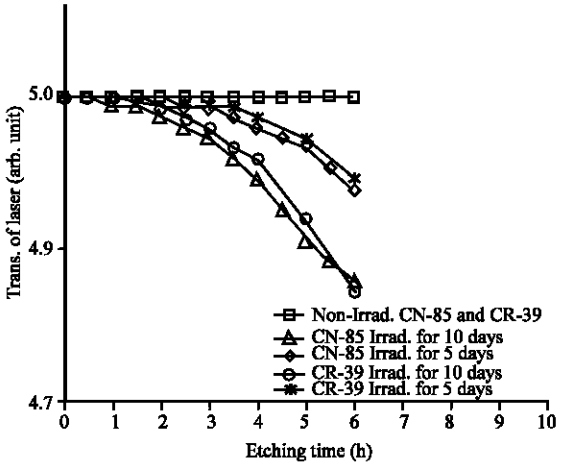

Fig. 13: Transmission of laser light through the SSNTDs irradiated by neutrons (Al-Saad and Abbas, 2001)

mentioned before, the actualities of oblique conical tracks and their optical properties have been previously explained by Groetz *et al.* (1998).

Neutron and alpha particles etched tracks evaluation using He-Ne laser: Groetz's proposals developed the applications of coherent light for evaluating more features of etched tracks. Al-Sàad *et al.* (2001) attempted to apply He-Ne laser light to investigate nuclear tracks of ^{241}Am alpha particles and Am-Be neutrons, registered by 250 μm CR-39 and 100 μm CN-85 foils (Al-Sàad and Abbas, 2001). A photodiode was used as a light detector at distance of 10 cm from the SSNTDs for measuring light scattered by track apertures.

Figure 12 shows the behavior of light transmission through the CR-39 and CN-85 foils in the normal incidence case (0°) versus chemical etching time. Apart from non-irradiated foils which have very low track densities as the natural background, in both cases of alpha and neutron irradiation with short irradiation time (2 h and 5 days for alpha particles and neutron, respectively) there is a mild decrease in the light transmission due to increasing of etching time. In both cases (short and long irradiation) for alpha tracks, decreasing shown in transmitted light can be justified by considering track apertures growth due to increase of etch duration which can lead to an optical density decreasing (Eq. 8). However, the saturation phenomenon in track appearance can occur when the etch period continues to increase. On the other hand in the case of high level irradiation (94 h for alpha irradiation) there is significantly a decrease in light transmission which can occur due to tracks overlapping phenomenon. However, as shown in Fig. 13 deferent mechanism to generate fast-neutron-induced tracks in polymers can cause a different feature for mentioned curves. Since nuclear tracks are in fact the particular damages in polymeric structure of SSNTDs that are created by charged particles, neutrons (as electrical neutral particles) cannot directly be able to create primary latent tracks. Nonetheless, tracks are indirectly induced by neutrons based on creating of charged induced recoil-particles in the polymeric structure. On the other hand, the productive reactions of recoil-particles can occur anywhere inside the polymer volume along the neutrons trajectory, so there is no necessarily that the related polymeric destruction begins from the surface of polymer. Therefore, new tracks are likely to be created due to increase of etching time.

New advances: Confocal Laser Scanning Microscopy (CLSM) is one of the most significant advances in optical microscopy. This technique is able to visualize deeply within cells and tissues and collect sharply defined optical sections from which three-dimensional renderings can be created. Development of modern confocal microscopes has been especially accelerated by new advances in computer and storage technology, laser systems, detectors, interference filters and fluorophores for highly specific targets.

Recently, a lot of studies have been carried out to evaluate of the response of various SSNTDs using confocal laser scanning microscopy. This technique is especially beneficial in the case of track geometrical measurements for short etching times. In 1990, Petford and Miller (1990 and 1992) introduced CLSM to record and measure three-dimensional parameters of fission tracks in apatite which is impossible by ordinary transmitted light microscopes. As authors have mentioned, using technique of CLSM is particularly useful in the case of paleothermal studies and dating of

geologically young materials which require high speed equipment to measure and process large amounts of such materials. Therefore, using of the conventional microscopy to process the large amounts of materials in such studies can be extremely difficult and very expending time. The results of CLS microscopy are sharp and high resolution images with a very narrow depth of field. Furthermore, the method of CLSM is accompanied by computer programming to achieve required image analysing. Unlike other techniques such as SEM and TEM, the CLSM method enables to achieve a high magnification without special sample preparation (Petford and Miller, 1992).

In 2000, Fromm *et al.* (2000) introduced a method based on CLSM to evaluate the bulk and track etch-rates (V_b and V_t, respectively) using electrochemical etching process of CR-39 foils. As the authors mentioned, all previous methods to evaluate SSNTDs response to the etching condition expend a very long time. However, a method based on CLSM offers 3-D high resolution images which enable tracks analysis one by one. Therefore, as Chambaudet *et al.* (2000) have mentioned, the methods based on optical microscopy is usually applied for the long etching times. They also used CLSM in fluorescent mode to measure the geometrical parameters (diameter and length) of Li tracks in CR-39 after applying a staining method by fluorochorome. As they discussed the advantages of this method are accuracy, 3-D imaging, automatic measurements etc. Meesen and Van Oostveldt (1997) Jakes *et al.* (1997); Vaginay *et al.* (2001); Fromm *et al.* (2001); Meesen and Poffijn (2001) and Fromm *et al.*, 2003) also used the method based on CLSM to evaluate of various kinds of SSNTD's responses using three-dimensional visualization techniques (Fig. 3).

CONCLUSIONS AND SUGGESTIONS

As it described, many researchers have attempted to apply theoretical and experimental methods of modern optics to demonstrate a fair relationship between optical properties of nuclear tracks and their geometrical parameters in polymeric detectors. For instance, using the Fourier transformation method, Palacios *et al.* (2001) showed that there is a measurable correlation between peaks of Fourier spectrum and track diameters. They also found out a linear relationship between number of tracks having a specific diameter and the secondary harmonic amplitude demonstrating the same diameters (Eq. 16 and 17). The proposed method by researchers based on modern optics allows obtaining many track parameters such as density, diameter including minor and major diameter, incidence angle and occasionally track length in some particular cases.

Many studies mentioned above show that nuclear track evaluations using the recent developed methods based on modern optics can be applicable and accurate as well as the conventional methods. The methods mentioned above have caused a revolution to improve the applications of Solid State Nuclear Track Detectors (SSNTDs) particularly if they are accompanied by computer simulation and image processing techniques. Therefore, we propose applying further computer simulations and image processing techniques to access more appropriate optical images. Such preparations help researchers to apply some techniques which can lead to more accurate estimating of particle characteristics. Optics of nuclear tracks includes some further aspects such as evaluation about tracks counting under the normal and noisy fields, track diameters and depth determination, tracks obliquity phenomenon, double and triple tracks, comparison between automated measurements and manual performances, etc. Besides, different mechanisms of track formation by various particles may be perused applying optics of nuclear tracks. A perfect example to clarify this subject is the completely different mechanisms of tracks producing by charged particles and fast neutrons as the neutral particles. We know also that there are fundamental differences between methods of track production by fast-neutron-induced-recoils and whatever called thermal neutron registration by applying particular converters such as ^{10}B. The mentioned matter is important because it can cause much problematic identification in neutron measurements. In some simulation models such as Groetz's work described in this review article, more appropriate parameters such as sufficient track values (more than 1000 tracks) should be considered to provide easier access to accurate calculation. Furthermore, it seems to be necessary to apply more image processing techniques such as histogram processing, image smoothing and sharpening like using the derivative filters to decrease technical deficiencies in track-shape recognition which can cause less accurate measurements. Further investigations not only lead researchers to know further about optical aspects of solid state nuclear track detectors, but even may be applied as a proper alternative method for radiation dosimetry in the future.

ACKNOWLEDGMENT

The authors would like to express their thanks to Professor Lei Huo for his kindly advice during the preparing of this article.

REFERENCES

Al-Sàad, A.A. and S.J. Abbas, 2001. He-Ne laser transmission through etched CR-39 and CN-85 detector containing alpha- and neutron-induced tracks. Radiat. Meas., 34: 91-93.

Born, M. and E. Wolf, 1959. Principles of Optics. Pergamon Press, Oxford.

Chambaudet, A., M. Fromm, G. Meesen, A. Poffijn and F. Vaginay, 2000. Using a confocal microscope for the extraction of track parameters in CR-39 SSNTDs. In: Proceeding of the The 20th International Conference on Nuclear Tracks in Solids, August 28-September 1 2000, Portoro, Slovenia.

Ditlov, V., 1995. Calculated tracks in plastics and crystals. Nucl. Tracks Radiat. Meas., 25: 89-94.

Durrani, S.A. and R.K. Bull, 1987. Solid State Nuclear Track Detection. Pergamon Press, Oxford.

Fews, A.P., 1986. Fully automated image analysis of alpha particle and proton etched tracks in CR-39. Nucl. Tracks, 12: 221-225.

Fews, A.P., 1992. Flexible analysis of etched nuclear particle tracks. Nucl. Instr. Meth., B72: 91-103.

Fleischer, R.L., P. B. Price and R.M. Walker, 1975. Nuclear Tracks in Solids. University of California Press, Berkeley.

Fromm, M., F. Vaginay, G. Meesen, A. Chambaudet and A. Poffijn, 2001. 3-D confocal microscopy of etched nuclear tracks in CR-39. Phys. Medica. XVII, Suppl. 1: 144-146.

Fromm, M., F. Vaginay, G. Meesen, A. Chambaudet and A. Poffijn, 2003. Watching at the correlation between the specific track-etch rate and the primary physical parameters of the swift ion interaction with the CR-39. Radiat. Meas., 36: 93-98.

Groetz, J.E., A. Lacourt and A. Chambaudet, 1998. Coherent light scattering by nuclear etched tracks in the PADC (a form of CR-39). Nucl. Inst. Methods Phys. Res., B142: 503-514.

Groetz, J.E., A. Lacourt, P. Meyer, M. Fromm, A. Chambaudet and J. Potter, 1999. A new method for reading CR-39 by using coherent light scattering. Radiat. Prot. Dosim., 85: 447-450.

Heinrich, W., C. Brechtmann, J. Dreute and D. Weidmann, 1988. Applications of plastic nuclear track detectors in heavy ion physics. Nucl. Tracks Radiat. Meas., 15: 393-402.

Ilić, R. and M. Najer, 1990a. Image formation in track-etch detector I. The large area signal transfer function. Nucl. Tracks Radiat. Meas., 17: 453-460.

Ilić, R. and M. Najer, 1990b. Image formation in track-etch detector II. The space-dependent transfer function in thin detectors. Nucl. Tracks Radiat. Meas., 17: 461-468.

Ilić, R. and M. Najer, 1990c. Image formation in track-etch detector III. The space-dependent transfer function in thick detectors. Nucl. Tracks Radiat. Meas., 17: 469-473.

Jakes, J., P. Gais and J. Voigt, 1997. Electrochemically etched tracks by means of confocal microscopy. Radiat. Meas., 28: 853-856.

Meesen, G. and P. Van Oostveldt, 1997. Use of a CSLM for the analysis of chemical etched tracks in PADC. Radiat. Meas., 28: 845-848.

Meesen, G. and A. Poffijn, 2001. Semi-automated analysis of three-dimensional track images. Radiat. Meas., 34: 161-165.

Moore, M.E., H.J. Gepford, R.E. Hermes, N.E. Hertel and R.T. Devine, 2002. Laser Illuminated Etched Track Scattering (LITES) dosimetry system. Radiat. Prot. Dosim., 101: 43-45.

Palacios, D., F. Palacios, L. Sajó-Bohus and J. Palfalvi, 2001. A new method to measure track density and to differentiate nuclear tracks in CR-39 detectors. Radiat. Meas., 34: 119-122.

Petford, N. and J.A. Miller, 1990. SLM confocal microscopy: An improved way of viewing fission tracks. J. Geolog. Soc., 147: 217-218.

Petford, N. and J.A. Miller, 1992. Three-dimensional imaging of fission tracks using confocal scanning laser microscopy. Am. Mineral., 77: 529-533.

Price, P.B. and R.M. Walker, 1962. Chemical etching of charged particles. J. Applied Phys., 33: 3407-3412.

Skvarč, J., R. Ilić and A. Korde, 1992. Digital evaluation of ^{6}Li (n, α) reaction product tracks in CR-39 detector. Nucl. Instr. Meth., B 71: 60-64.

Skvarč, J., 1997. The influence of mechanical stresses on etching of charged particle tracks in CR-39 polymer. Dissertation, University of Ljubljana, Ljubljana (In Slovene).

Skvarč, J., 1999. Optical properties of individual etched tracks. Radiat. Meas., 31: 217-222.

Somogyi, G., I. Hunyadi, A.F. Hafez and G. Espinosa, 1984. A new possibility for high resolution spectroscopy of nuclear particles entering CR-39 at selected dip angles. Nucl. Tracks Radiat. Meas., 8: 163-166.

Tommasino, L., 1970. Electrochemical etching of damage track detectors by H.V. pulse and sinusoidal wave forms, CNEN Report RT/PROT, Vol. 1.

Tommasino, L., 1993. Importance of track detectors in radiation dosimetry. Nucl. Tracks Radiat. Meas., 22: 707-717.

Tüke, B., G. Seger, M. Acchatz and W.V. Seelen, 1978. Fourier optical approach to the extraction of morphological parameters from the diffraction pattern of biological cells. Applied Opt., 17: 2754-2761.

Vaginay, F., M. Fromm, D. Pusset, G. Meesen, A. Chambaudet and A. Poffijin, 2001. 3-D confocal microscopy track analysis: A promising tool for determining CR-39 response function. Radiat. Meas., 34: 123-127.

Yu, F.T.S., 1983. Optical Information Processing. John Wiley and Sons.